

# Modeling and Investigation of Multilayer Piezoelectric Transformer with a Central Hole for Heat Dissipation

Vo Viet Thang\*, Insung Kim<sup>†</sup>, Soonjong Jeong\*\*, Minsoo Kim\*\* and Jaesung Song\*\*

**Abstract** – A multilayer square-type piezoelectric transformer with a hole at the center was investigated in this paper. Temperature distribution at the center was improved by using this construction, therefore increasing input voltage and output power. This model was simulated and investigated successfully by applying a finite element method (FEM) in ATILA software. An optimized structure was then fabricated, examined, and compared to the simulation results. Electrical characteristics, including output voltage and output power, were measured at different load resistances. The temperature distribution was also monitored using an infrared camera. The piezoelectric transformer operated at first radial vibration mode and a frequency area of 70 kHz. The 16 W output power was achieved in a three-layer transformer with 96% efficiency and 20 °C temperature rise from room temperature under 115 V driving voltage, 100 Ω matching load, 28 x 28 x 1.8 mm size, and 2 mm hole diameter. With these square-type multilayer piezoelectric transformers, the temperature was concentrated around the hole and lower than in piezoelectric transformers without a hole.

**Keywords:** Central hole, Heat dissipation, Multilayer piezoelectric transformer, Simulation, Temperature distribution, Thermal reduction

## 1. Introduction

Based on piezoelectric materials, piezoelectric transformers were invented as a combination of an actuator and a transducer which have been used widely with the name of Rosen-type transformer. While conventional magnetic transformers use a magnetic field as a medium for energy transformation, piezoelectric transformers utilize a mechanical vibration with advantages such as higher efficiency, miniaturization, absence of electro-magnetic noise, and nonflammability [1–5]. These benefits have led piezoelectric transformers to be studied and applied in the development of smart grid and green technology to meet requirements such as effective energy utilization, reduction of global warming, and environmental protection. These transformers can be used for DC/AC or AC/DC converters, battery chargers, power supply for display, and air cleaners. Although rectangular-shaped Rosen-type piezoelectric transformers are still being applied for step-up commercial applications, various types of piezoelectric transformers using different vibration modes have been proposed and developed to obtain higher power and smaller size [6–10].

Finite Element Method (FEM) and electro-mechanical lumped equivalent circuit model have been used to analyze piezoelectric transformers. Many significant design

aspects such as shape, electrode pattern, and electrode position, can only be investigated with the FEM technique. FEM modeling efforts for piezoelectric transformers have been studied on the Rosen-type, ring-shaped type, circular type, and unipolar disk-type using software such as ATILA, ANSYS, and NTUPZE [11–15]. ATILA was utilized effectively in the simulation of new piezoelectric transformers due to its simplifications in importing data and showing results [16].

One of the most important factors affecting piezoelectric transformers is temperature; hence, piezoelectric material and construction should be improved to obtain transformers with higher power at lower normal temperature increase. Internal losses are the heat generated which leads to the increased temperature of piezoelectric transformers, especially in high power, and the change in transformer characteristics. In previous research reports, the effects of temperature on piezoelectric material parameters were mentioned, but temperature distribution was not focused on [17].

In this work, the modeling of a square-shaped multilayer step-down piezoelectric transformer with a central hole before the fabrication was studied using ATILA software. First, the parameters of hard piezoelectric ceramic were measured from fabricated specimens and inserted into the simulation. The effects of frequency and load resistance on the electrical properties were also studied. Temperature investigation at different load resistances and temperature distribution were carried out. Thus, the electrical properties and temperature of step-down piezoelectric transformers

<sup>†</sup> Corresponding Author: Battery and Piezoelectric Research Center, KERI, Changwon, Korea. (kimis@keri.re.kr).

\* Department of Energy Conversion, University of Science and Technology, Daejeon, Korea. (thangvbk@ust.ac.kr).

\*\* Battery and Piezoelectric Research Center, KERI, Changwon, Korea  
Received: August 3, 2010; Accepted: March 24, 2011

conforming with the simulation fabricated by piezoelectric ceramics were measured and compared to the simulated results.

## 2. Simulation and Experiment

The schematic diagram of a multilayer piezoelectric transformer with a hole at the center for improved thermal distribution is presented in Fig. 1. In this structure, an input part has one layer, while an output part includes three layers; as a result, a low output voltage is obtained. These parts are symmetric and divided by a 1.5 mm-width isolation gap. Poling direction along with the thickness direction is indicated by arrows. Electrodes of the output part are connected by two symmetric corners to make an advanced electrode pattern. When exciting a voltage to the input part, the radial vibration is generated and transferred to the output part by the converse piezoelectric effect. The mechanical energy is then converted into electrical energy by the direct piezoelectric effect. In this diagram, the transformer model was created by GiD software, which was associated with ATILA for the calculation process. From the four-sided areas, volumes were extruded and managed with a layer function necessary to the next steps. Conditions in simulating the transformer consisted of piezoelectric ceramic with measured parameters, electrical potential (input voltage, ground, and load resistance), and polarization direction. Apart from such conditions, the thermal analysis required thermal coefficients of the material and convection factors of areas surrounding the piezoelectric transformer. The electrical boundary condition and poling direction are presented in Fig. 2. After meshing the model systemically in 168 hexahedral elements and 1082 nodes, a modal analysis was used to find the resonance area. Harmonic analysis was then selected to investigate the transformer characteristics in this frequency area. The calculation process was carried out by ATILA software with the data transferred from GiD pre-processing, and then the results performed in GiD post-processing. Output voltage, temperature, admittance, and impedance characteristics were displayed, and output power and temperature rise were calculated. From the simulation of difference in hole diameter and thickness, the output power and temperature rise were evaluated to choose an appropriate transformer size.

A piezoelectric transformer similar to the simulation with a 28 x 28 x 1.8 mm size and a 2 mm hole diameter was fabricated using a hard piezoelectric ceramic because of high electromechanical factor and low energy loss. Commercial-grade raw powders (Junsei Chemical Co., Ltd) of PbO (99%), ZrO<sub>2</sub> (99%), TiO<sub>2</sub> (98%), NiO (99%), Nb<sub>2</sub>O<sub>5</sub> (99.5%), and MnO<sub>2</sub> (99%) were used as raw materials to prepare the ceramics, with the composition of 0.01Pb(Ni<sub>1/3</sub>Nb<sub>2/3</sub>)O<sub>3</sub>-0.08Pb(Mn<sub>1/3</sub>Nb<sub>2/3</sub>)O<sub>3</sub>-0.91Pb(Zr<sub>0.505</sub>Ti<sub>0.495</sub>)O<sub>3</sub> (abbreviated as PNN-PMN-PZT). Excess powders of 0.3wt% PbO and

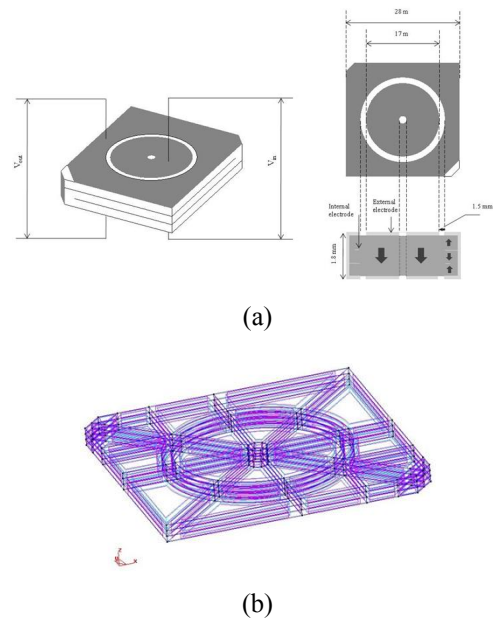


**Fig. 1.** Schematic diagram of the multilayer piezoelectric transformer: (a) dimensions of the three-layer piezoelectric transformer; (b) model in simulation.

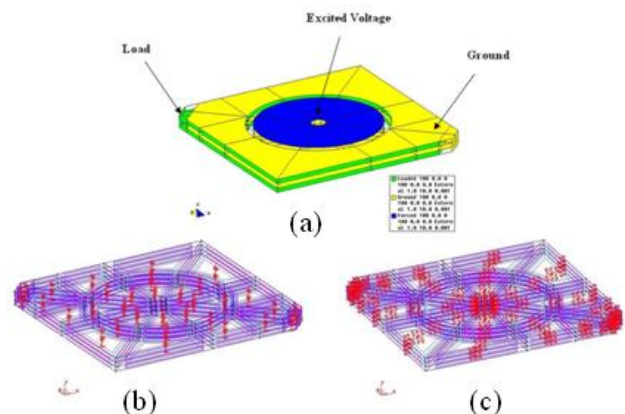


**Fig. 2.** Conditions of the simulation: (a) boundary condition; (b) poling direction, and (c) convictional surface

0.3wt% Nb<sub>2</sub>O<sub>5</sub> were added to the stoichiometric composition. The excess Nb<sub>2</sub>O<sub>5</sub> in PZT ceramic improves electromechanical coupling coefficient and dielectric loss because of its extrinsic contribution for internal mechanical friction [18]. The ceramic powder was mixed with solvent and 1 wt% dispersant by ball-mill method for 24 h, and then 8 wt% polyvinyl butyral and 4 wt% dibutyl phthalate were added to make slurry for a tap-casting process. An 80 mm-thick green tape was made using a casting machine with a doctor blade and then dried prior to cutting in sheets and punching four corners to fix the position for the next steps. Internal electrodes were printed using Ag/Pd paste. The sheets were stacked under suitable pressure and temperature to obtain cohesion and desired thickness. The

plate was cut to obtain separated samples before punching a hole at the center.

After the burn-out process, samples were sintered at 1150 °C for four hours in a sealed alumina crucible with lead medium. The samples were ground at all sides, polished to make a connecting corner, and printed with external electrodes. Wires were soldered to electrodes before poling piezoelectric transformers in a silicon oil bath at 120 °C under a 3 kV/mm DC voltage.

Fig. 3 shows a diagram measuring the electrical properties of the piezoelectric transformer that consists of a function generator, a power amplifier, and an oscilloscope. Temperature was determined using an infrared camera after an operating period of 20 min. An HP4294A impedance analyzer was used to investigate the piezoelectric properties of the piezoelectric transformer.

### 3. Results and Discussion

Based on the successful simulation of multilayer piezoelectric transformer on GiD-ATILA software, the thickness and hole diameter changed while the surrounding size remained at 28 x 28 mm. Characteristics, including output voltage and temperature as a function of different hole diameters and thicknesses as shown in Fig. 4, were evaluated to select a suitable dimension. Temperature and output voltage increased with a decrease in thickness, but decreased with an increase in hole diameter. With the desired output voltage, normal temperature, and suitable fabrication, the piezoelectric transformer with 0.6 mm thickness and 2 mm hole diameter was chosen. Afterward, the transformer characteristics were simulated and investigated specifically. From Fig. 5(a), in the frequency range of 60–90 kHz of output impedance curve, the resonance frequency area of the multilayer piezoelectric transformer was around 70 kHz, and the minimum impedance was 2.11 Ω at the resonance frequency of 67.9 kHz. In the experimental impedance curve, this impedance was 3.61 Ω at the resonance frequency of 70.2 kHz, as shown in Fig. 5(b). From the impedance analysis, the matching impedance was 100 Ω.

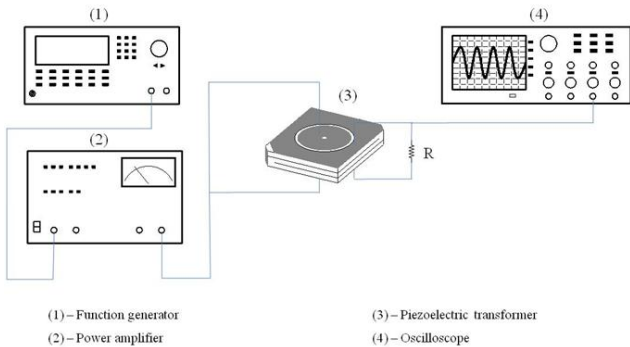


**Fig. 3.** Schematic of the setup for measuring electric characteristic

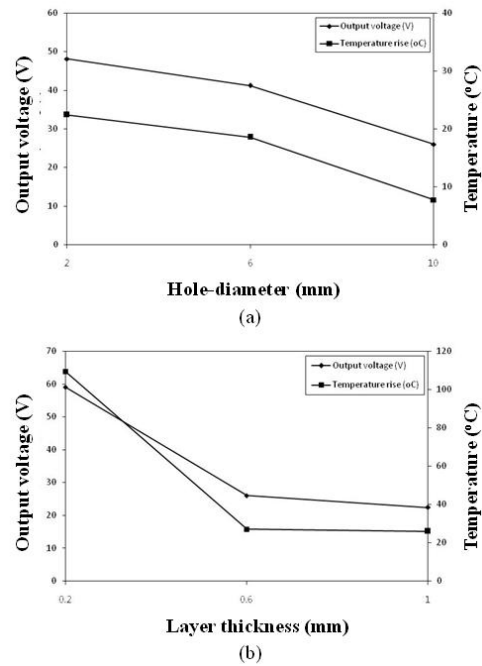


**Fig. 4.** Output voltage and temperature rise as a function of hole diameter and thickness: (a) different hole diameters; (b) different thicknesses.

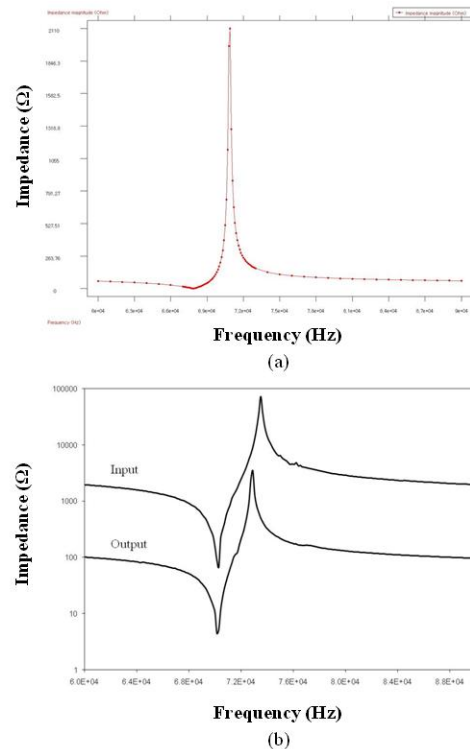


**Fig. 5.** Impedance curves of the multilayer piezoelectric transformer: (a) in the simulation; (b) in the experiment.

Fig. 6 shows output voltage as a function of frequency at different load resistances under a constant input voltage of 100 V in the ATILA simulation and experiment. The

driving frequencies describing the maximum output voltage were near resonance frequency as mentioned above and increased with the increasing of the load resistance. Output voltage rose gradually when the load resistance went up because of the faster molecular alternation in the transformer. Maximum output voltages of the multilayer transformer at the driving frequency of 69–72 kHz in the simulation were 33.57, 48.33, 65.26, and 82.54 V at the load resistances of 50, 100, 150, and 200 Ω, respectively. These values in the experiment were 27.8, 32.4, 41.8, and 51.4 V, respectively. Reasons for the difference of output voltages could be the central deflection of the hole and the soldering position of the electric wire associated with the input section in the fabrication. In addition, electrode dimensions, electrode material, external connection of the electrodes, and real degree of texture due to poling were not considered; load resistance was also of concern as a distributed parameter depending on the total number of elements in the modeling [17, 19–20]. The difference of resonance frequencies between the simulated and experimental results was 5%, but this error was very small therefore, a forced cooling method at the center of transformer is more effective. This result is shown in Fig. 7.

Temperature rise as a function of input voltage and load resistance is presented in Fig. 8 after operating for 20 min. At low input voltage, the temperature changed slowly and differences between load resistances were small. From 80 V input voltage, the temperature increased more quickly, especially at 200 Ω due to high distinction compared to the matching load of 100 Ω. As shown in Fig. 9(a), in the

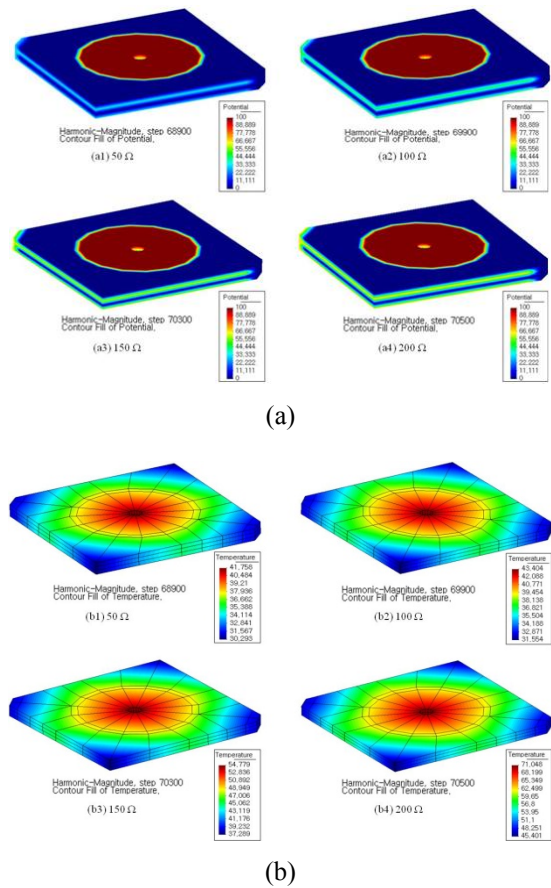


Fig. 7. Potential and temperature profile in three-dimension (3D) according to load resistance at resonance frequency: (a) potential profile; (b) temperature profile.

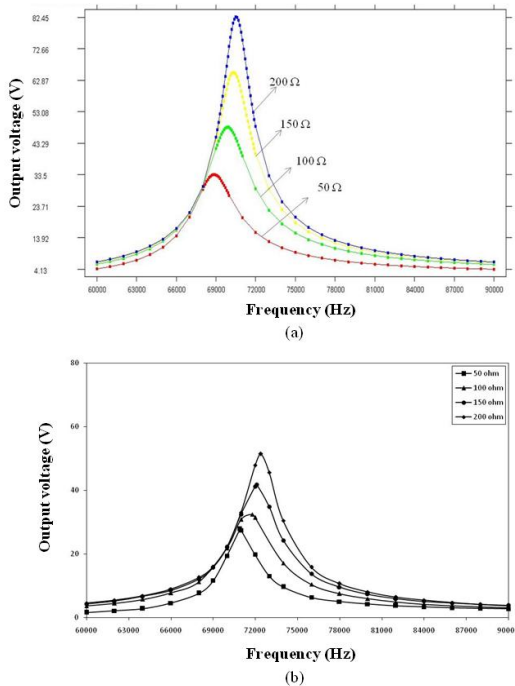


Fig. 6. Output voltage as a function of load resistance and frequency: (a) in the simulation; (b) in the experiment.

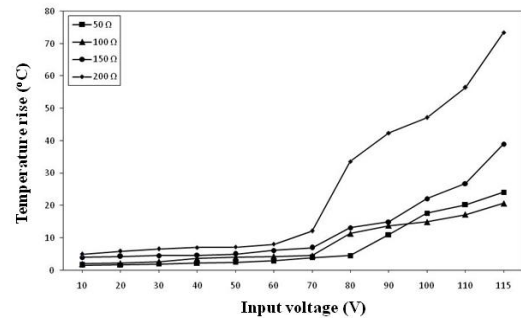
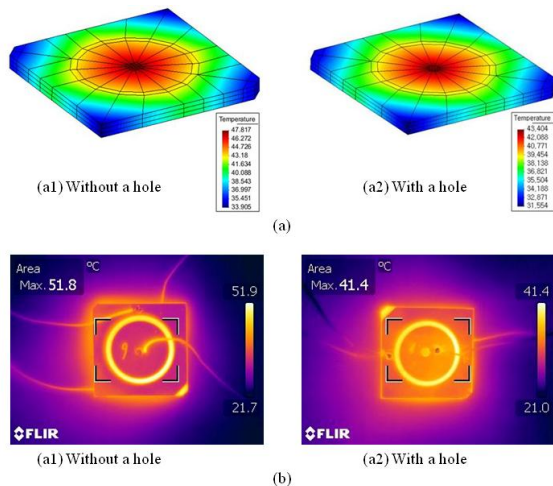


Fig. 8. Temperature rise as a function of input voltage and load resistance

simulation, the piezoelectric transformer with a hole at the center was more effective in reducing the temperature under the 115 V input voltage than the piezoelectric transformer without a hole. Furthermore, temperature distributions of fabricated transformers were captured using an infrared camera at such conditions in Fig. 9(b). The highest temperature of transformers with a hole was 41.4 °C, while this value was 51.9 °C at the non-hole



piezoelectric transformer. The non-electrode surface and the increase of the hole area in the transformer improved the heat-transferring ability. This captured temperature distribution was different from the 3D simulation results because of the emissivity between electrodes and piezoelectric material in the practical experiment. With a large electrode area, the thermal emission ability of the printed electrode material needs to be improved to obtain better temperature distribution.



**Fig. 9.** Comparison of temperature distribution: (a) in the simulation; (b) in the experiment.

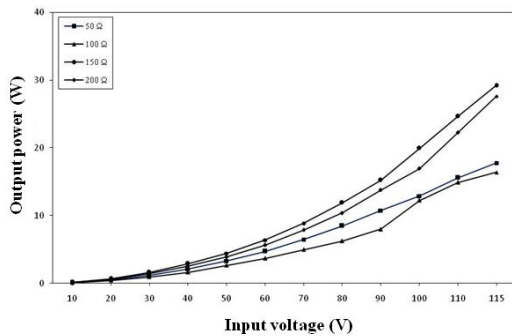


**Fig. 10.** Output power as a function of input voltage and load resistance

The output powers as a function of input voltage and load resistance of the multilayer piezoelectric transformer are described in Fig. 10. When the input voltage increased, output power increased sharply due to a quadratic dependence of output voltage. Input voltage was only determined up to 115 V because the temperature rise soared from this point in our measurement of piezoelectric transformers. The output power of 16 W was achieved stably at the load resistance of 100  $\Omega$  because the temperature rise was about 20  $^{\circ}\text{C}$  in the previous temperature analysis and the efficiency was 96%.

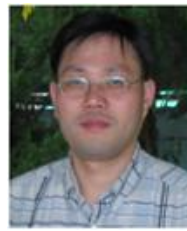
## 4. Conclusion

Heat dissipation was improved in the square-shaped three-layer piezoelectric transformer with a central hole and a  $28 \times 28 \times 1.8$  mm size in both the modeling using FEM method and the fabrication. Based on this structure, the aspects affecting the operation of the piezoelectric transformer were investigated. The piezoelectric transformer was operated at the resonance frequency of the first radial vibration mode. In contrast to the conventional multilayer piezoelectric transformer without a hole, temperature reduction was obtained in the piezoelectric transformer with a hole at the center. Thus, output power was 16 W at a stable operating condition at 115 V input voltage and 100  $\Omega$  load resistance, and this piezoelectric transformer could be used in AC/DC converters to light LED systems. Improve the method for making the central hole and simulating more appropriate electrodes, as well as the degree of texture according to practical piezoelectric transformers, are the future directions of this study.

## References

- [1] V. V. Thang, I. S. Kim, H. K. Joo, J. S. Song, S. J. Jeong, and M. S. Kim, "Investigation of the Optimum Design for a 10 W Step-down 3-layer Piezoelectric Transformer", *J. Korean Phys. Soc.*, 58, pp. 622-626, 2011.
- [2] K. J. Lim, S. H. Park, O. D. Kwon, and S. H. Kang, *KIEE Inter. Trans. Elec. App.*, 5-C, 102 (2005).
- [3] H. K. Joo, I. S. Kim, J. S. Song, S. J. Jeong, and M. S. Kim, *J. Korean Phys. Soc.*, 56, 374 (2010).
- [4] I. S. Kim, H. K. Joo, S. J. Jeong, M. S. Kim, and J. S. Song, *Phys. Status Solidi.*, 7, 2331 (2010).
- [5] I. S. Kim, H. K. Joo, J. S. Song, S. J. Jeong, and M. S. Kim, *J. Korean Phys. Soc.*, 57, 963 (2010).
- [6] S. Priya, S. Ural, H. W. Kim, K. Uchino, and T. Ezaki, *Jpn. J. Appl. Phys.*, 43, 3503 (2004).
- [7] P. Laoratanakul and K. Uchino, *Appl. Ferroelect.* 2004. ISAF-04. 2004 14th IEEE Inter. Symp., 229 (2004).
- [8] I. S. Kim, H. K. Joo, S. J. Jeong, M. S. Kim, J. S. Song, and V. V. Thang, *J. Korean Phys. Soc.*, 58, 627 (2011).
- [9] I. S. Kim, M. S. Kim, S. J. Jeong, J. S. Song, H. K. Joo, V. V. Thang, and A. Muller, *J. Korean Phys. Soc.*, 58, 580 (2011).
- [10] S. Priya, H. Kim, S. Ural, and K. Uchino, *IEEE Trans. Ultrason., Ferroelect., Freq. Contr.*, 53, 810 (2006).
- [11] Y. J. Yang, C. C. Chen, Y. M. Chen, and C. K. Lee, *J. Chin. Inst. Eng.* 31, 925 (2008).
- [12] H. L. Li, J. H. Hu, and H. L. W. Chan, *IEEE Trans. Ultrason., Ferroelect., Freq. Contr.*, 51, 1247 (2004).
- [13] E. Heinonen, J. Juuti, and S. Leppävuori, *J. Eur. Ceram. Soc.*, 25, 2467 (2005).

- [14] S. T. Ho, IEEE Trans. Ultrason., Ferroelect., Freq. Contr., 54, 2110 (2007).
- [15] T. Tsuchiya, Y. Kagawa, N. Wakatsuki, and H. Okamura, IEEE Trans. Ultrason., Ferroelect., Freq. Contr., 48, 872 (2001).
- [16] B. Koc, Y. Gao, and K. Uchino, Jpn. J. Appl. Phys. 42, 509 (2003).
- [17] H. W. Yoo, C. H. Lee, J. S. Rho, and H. K. Jung, IEEE Trans. Ultrason., Ferroelect., Freq. Contr., 53, 8 (2006).
- [18] S. J. Yoon, J. W. Choi, J. Y. Choi, D. D. Wan, Q. Li, and Y. Yang, J. K. Phys. Soc. 57, 863 (2010).
- [19] A. M. Sanchez, M. Sanz, R. Prieto, J. A. Oliver, P. Alou, and J. A. Cobos, IEEE Trans. Ind. Electron., 55, 1 (2008).
- [20] J. L. Jones, B. J. Iverson, and K. J. Bowman, J. Am. Ceram. Soc., 90, 2297 (2007).



**Soonjong Jeong** received his Ph.D. degree in Material Science and Engineering from the University of Washington, Washington, USA, in 2000. He joined UST as an Associate Professor in the Material Department. His research interests are piezoelectric ceramics and devices.



**Minsoo Kim** received his Ph.D. degree in Material Science and Engineering from KAIST, Daejeon, Korea in 2005. He is currently a senior researcher in KERI. His research interests are lead-free piezoelectric ceramics and devices.



**Vo Viet Thang** received his B.S. degree in Electrical Engineering from Hanoi University of Science and Technology, Hanoi, Vietnam, in 2009. He is currently an M.S. student in the University of Science and Technology (UST), Daejeon, Korea, and conducting research in the Battery and Piezoelectric

Research Center of Korea Electrotechnology Research Institute, Changwon, Korea. His research interests include designs and simulations of piezoelectric devices.



**Jaesung Song** received his Ph.D. degree in Material Science and Engineering from KAIST, Daejeon, Korea, in 1991. He is presently an associate professor in the Energy Conversion Department of UST. His research interests are ferroelectric material and piezoelectric devices.



**Insung Kim** received his Ph.D. degree in Electrical Engineering from Pusan University, Pusan, Korea, in 2003. He is currently a researcher in KERI and an Associate Professor in the Energy Conversion Department of UST. His research interests are ferroelectric materials, piezoelectric harvesting and

devices.